Life Sciences 239 (2019) 116935

Contents lists available at ScienceDirect

Life Sciences

journal homepage: www.elsevier.com/locate/lifescie

Gastrodin combined with rhynchophylline inhibits cerebral ischaemia-induced inflammasome activation via upregulating miR-21–5p and miR-331–5p

Heng-Sheng Zhang[a,1], Mei-Fang Liu[a,1], Xiong-Ying Ji[b], Chang-Rong Jiang[c], Zi-Li Li[c], Bo OuYang[a,*]

[a] Department of Traditional Chinese Medicine Rehabilitation, Affiliated Nanhua Hospital, University of South China, Hengyang, 421002, Hunan Province, PR China
[b] Department of Gastroenterology, Affiliated Nanhua Hospital, University of South China, Hengyang, 421002, Hunan Province, PR China
[c] Department of Cardiology, Affiliated Nanhua Hospital, University of South China, Hengyang, 421002, Hunan Province, PR China

ARTICLE INFO

Keywords:
Gastrodin
Inflammasome
miR-21–5p
miR-331–5p
Rhynchophylline

ABSTRACT

Background: The protective effects of gastrodin and rhynchophylline in ischaemic injury have been reported. However, the underlying mechanism and the effect of the combination of these two drugs in ischaemic injury remain unclear. Herein, we aimed to explore the effects of the combination of gastrodin and rhynchophylline on ischaemia-induced inflammasome activation as well as the underlying mechanism.

Methods: Middle cerebral artery occlusion (MCAO) mice and oxygen glucose deprivation (OGD)-treated BV2 cells were used as *in vivo* and *in vitro* models of ischaemia, respectively. Cerebral injury was determined by TTC staining, H&E staining and neurological deficit scores. The effects of the combination of gastrodin and rhynchophylline on inflammasome activation were measured by the MTT assay, Western blotting and ELISA. The expression of miR-21–5p and miR-331–5p was measured by qRT-PCR. The potential binding between miR-21–5p and TXNIP and between miR-331–5p and TRAF6 was analysed with Targetscan and a luciferase assay.

Results: MCAO-induced tissue infarction, neurological deficits, inflammasome activation, and downregulation of miR-21–5p and miR-331–5p were all mitigated by the combination of gastrodin and rhynchophylline. In OGD-treated BV2 cells, the combination of gastrodin and rhynchophylline also alleviated inflammasome activation and restored the expression of miR-21–5p and miR-331–5p. TXNIP and TRAF6 were confirmed to be targets of miR-21–5p and miR-331–5p, respectively. Moreover, OGD-induced inflammasome activation was attenuated by the overexpression of either miR-331–5p or miR-21–5p and was further attenuated by the overexpression of both. Finally, we demonstrated that a miR-21–5p inhibitor and/or a miR-331–5p inhibitor counteracted the protective effects of gastrodin and/or rhynchophylline.

Conclusions: The combination of gastrodin and rhynchophylline exerts neuroprotective effects by preventing ischaemia-induced inflammasome activation via upregulating miR-21–5p and miR-331–5p.

1. Introduction

Globally, stroke is one of the most common causes of death and disability, accounting for approximately 12% of all deaths and 4.5% of all disability [11]. However, few drugs have been approved for the treatment of stroke. Accumulating evidence has highlighted the crucial role of neuroinflammation in the progression of stroke [3,7]. Recently, several studies have postulated that NOD-like receptor protein (NLRP3) signalling in microglia may be a crucial mediator of the inflammatory response in ischaemic stroke [22,24]. Once activated, NLRP3 recruits apoptosis-associated speck-like protein containing a CARD (ASC) and pro-caspase-1 to form the inflammasome complex, leading to the maturation of caspase-1 and the subsequent release of IL-1β and IL-18 [10]. IL-1β and IL-18 are both well-established initiators and mediators of the inflammatory response in stroke [9]. Furthermore, active caspase-1 can lead to pyroptosis, a unique type of programmed cell death, and to the initiation of the massive release of pro-inflammatory cytokines [5]. Consistently, several reports have indicated that the

* Corresponding author. Department of Traditional Chinese Medicine Rehabilitation, Affiliated Nanhua Hospital, University of South China, No. 336, Dongfeng South Road, Zhuhui District, Hengyang 421002, Hunan Province, PR China.
E-mail address: 1020192091@qq.com (B. OuYang).
[1] These are co-first authors.

https://doi.org/10.1016/j.lfs.2019.116935
Received 31 July 2019; Received in revised form 28 September 2019; Accepted 3 October 2019
Available online 11 October 2019
0024-3205/

inhibition of NLRP3 signalling alleviates ischaemia-induced brain injury in both *in vivo* and *in vitro* models [10,27]. As such, exploring novel strategies to target NLRP3 inflammasome activation in stroke may shed new light on stroke treatment.

Gastrodin, the active component of the Chinese herb tianma, has been widely used for epilepsy, headache, stroke and neurodegeneration diseases, including Alzheimer's disease [19]. Rhynchophylline, an alkaloid derived from the plant Uncaria, has long been used to improve central nervous system diseases, including numbness, convulsions and stroke [31]. The administration of both gastrodin and rhynchophylline has been reported to exert neuroprotective effects in both *in vivo* and *in vitro* models of ischaemic stroke; in MCAO mice, gastrodin ameliorates brain damage by activating the Akt/Nrf2 pathway and preventing apoptosis [23], and in rats, gastrodin alleviates ischaemia-induced injury by suppressing inflammation; [18]. Similarly, rhynchophylline attenuates ischaemic damage by suppressing the Toll-like receptor/NF-κB pathway [13]. However, as a classic "herb pair" (Chinese medicine herbal combination treatment), the effects of their combination on ischaemic stroke, especially ischaemia-induced inflammasome activation, remain unknown.

MicroRNAs are non-coding RNAs approximately 22 nucleotides in length [2]. They have been reported to play vital regulatory roles in cells by repressing the translation of protein-coding mRNAs via pairing with them [12]. miRNAs have been associated with the protective effects of multiple potential drugs derived from herbs in ischaemic stroke [8,29]. For example, magnesium lithospermate B protects the brain from ischaemic injury by modulating miR-107 [29], while ginsenoside Rg1 attenuates ischaemia-induced neuronal death via the miR-144/Nrf2 pathway [8]. miR-21 has been identified to mediate the beneficial effects of gastrodin in hypoxia-treated cardiomyocytes by regulating the PI3K/Akt pathway [25]. Meanwhile, miR-331 has been reported to play an essential role in the effects of rhynchophylline on resistance to ketamine addiction [17]. However, the roles of these two RNAs in the beneficial effects of gastrodin and rhynchophylline in cerebral ischaemia remain unclear.

Since microRNAs exert regulatory functions mainly through post-transcriptional repression, we used bioinformatics analysis to predict their targets. According to our Targetscan analysis, thioredoxin-interacting protein (TXNIP) is a target of miR-21–2p, while TNF receptor-associated factor 6 (TRAF6) is a target of miR-331–5p. TXNIP, an endogenous suppressor of thioredoxin, has been identified as an essential activator of the NLRP3 inflammasome by interacting with NLRP3 [32]. Meanwhile, TRAF6 promotes NLRP3 inflammasome activation by stimulating the assembly of NLRP3 and apoptosis-associated speck-like protein containing a CARD (ASC) [26]. Moreover, TRAF6 has been recognized to activate IKK and to thus activate NF-κB, resulting in an inflammatory response [21]. These findings suggest that gastrodin and rhynchophylline might ameliorate ischaemic brain injury by modulating TXNIP and TRAF6.

The present study aimed to clarify the effects of gastrodin combined with rhynchophylline on ischaemia-induced inflammasome activation as well as the underlying molecular details. Using MCAO mice and OGD-treated BV2 cells as ischemic models, we clearly show that gastrodin combined with rhynchophylline alleviates ischaemia-induced inflammasome activation by regulating miR-21–5p/TXNIP and miR-331–5p/TRAF6 and thus reveal a new therapeutic strategy for ischaemic stroke.

2. Materials and methods

2.1. Animal studies

All animal procedures were approved and supervised by the Research Ethics Committee of Affiliated Nanhua Hospital, University of South China. Sixty male C57BL/6 mice (8–10 weeks) were purchased from Hunan SJA Laboratory Animal Co., Ltd. (Hunan, China). These mice were randomly divided into 2 groups: the sham group and MCAO group. The MCAO procedure was carried out on a heating pad, and body temperature was maintained at 36.5–37.5 °C. After anaesthetising the mice, we isolated the right common carotid artery, the external carotid artery (ECA), and the superior thyroid artery. Then, a small incision was made in the ECA, and a 6-0 suture (Dermalon, 1741-11, Covidien, OH, USA) was introduced into the ECA and advanced to the middle cerebral artery. The artery was occluded for 1.5 h, and then the suture was removed to allow reperfusion. For the sham group, an identical procedure was performed without the introduction of the suture. After the MCAO procedure, the mice were randomly divided into four groups: mice intraperitoneally injected with gastrodin (100 mg/kg), rhynchophylline (30 mg/kg), both daily or the same volume of vehicle for 3 consecutive days (10 h, 34 h, and 58 h of reperfusion). Neurological deficits were evaluated using a modified neurological severity score (mNSS) scale on day 1 and day 3 after MCAO [20]. Then, the mice were sacrificed, and brain samples were collected for further analysis.

2.2. Triphenyl tetrazolium chloride (TTC) staining

Brain tissues were sectioned into 2-mm thick slices along the coronal plane. The slices were incubated in 2% TTC solution for 0.5 h in the dark and then fixed with 4% paraformaldehyde. Infarcted areas appeared white, while noninfarcted regions appeared pink. Finally, the slices were photographed and quantified with ImageJ software.

2.3. Haematoxylin and eosin (H&E) staining

Brian tissues were embedded in paraffin and sectioned into 30 μm-thick slices. Then, the slices were deparaffinized in xylene, dehydrated in ethanol, stained with haematoxylin for 7 min, washed with distilled water, immersed in 1% hydrogen chloride-ethanol solution for 3 s and counterstained in eosin for 20 s. Subsequently, the sections were dehydrated in a graded series of ethanol and xylene. Finally, the slices were mounted and photographed.

2.4. Cell culture

BV2 cells were purchased from Fuxiang Biotech (Nanjing, Jiangsu, China). The cells were maintained in DMEM medium (Gibco) containing 10% FBS (Gibco) at 37 °C in a 5% CO_2 incubator.

2.5. Transfection

miR-21–5p/miR-331–5p mimics or inhibitors were purchased from GenePharma (Shanghai, China). Transfection was performed with Lipofectamine 3000 (Life Technologies, Carlsbad, CA, USA) according to the manufacturer's instructions. Forty-eight hours after transfection, the cells were used for further experiments.

2.6. Oxygen glucose deprivation (OGD) model

BV2 cells were washed twice with PBS and incubated in glucose-free DMEM (Gibco). The cells were then placed in a chamber filled with a gas mixture of 95% nitrogen/5% carbon dioxide at 37 °C for the indicated duration. Then, the medium was replaced with fresh culture medium containing 10% FBS and penicillin/streptomycin, and the cells were transferred back to the 5% CO_2 incubator.

2.7. MTT assay

BV2 cells were plated into 96-well plates at an initial density of 10^4 cells per well. After OGD treatment, 25 μl of 1 mg/ml 3-(4,5-dimethyl-thiazol-2-yl)-2,5-diphenyltetrazolium bromide (MTT, Sigma Aldrich, St. Louis, MO, USA) was added to each well. Four hours later,

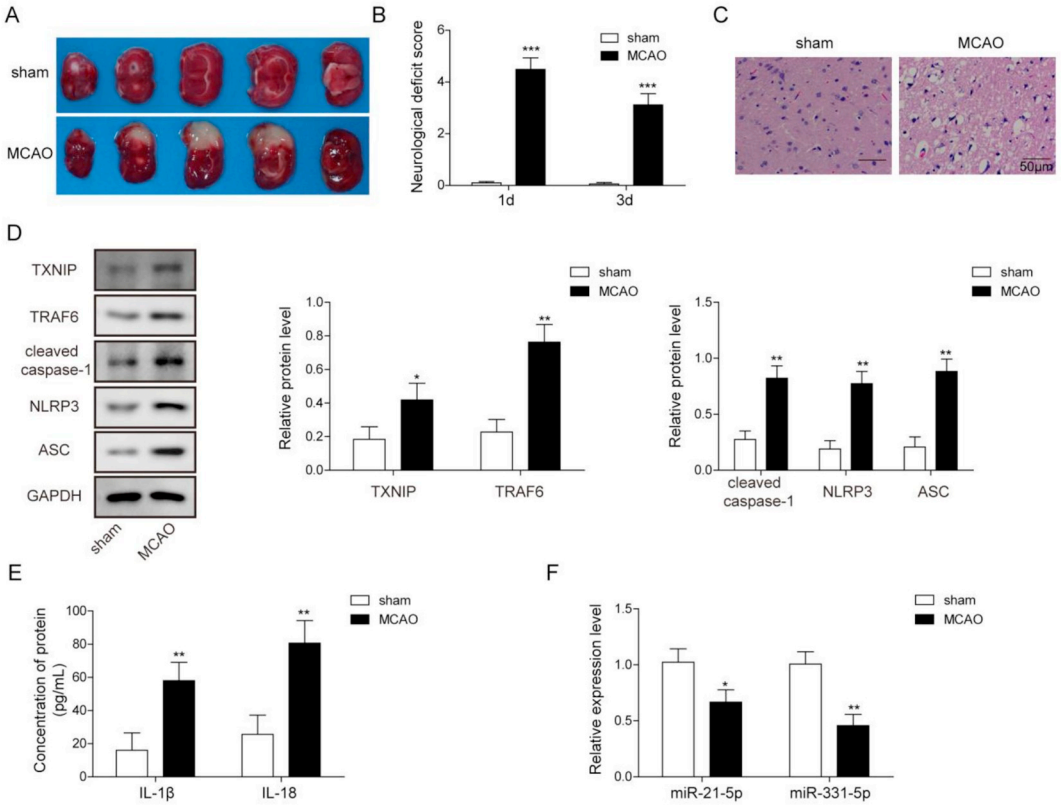

Fig. 1. Inflammasome activation was induced, and miR-21–5p and miR-331–5p were downregulated in MCAO mice. (A) Representative images of TTC of brain sections. Three days after I/R, brain sections were obtained for TTC staining. (B) Neurological deficits were determined by mNSS. The mNSS test was carried out on days 1 and 3 after I/R. (C) Representative images of H&E staining of brain sections. Three days after I/R, brain sections were obtained for H&E staining. (D) The expression levels of TXNIP, TRAF6, cleaved caspase-1, NLRP3 and ASC were examined by Western blotting on day 3 after I/R. (E) The levels of IL-1β and IL-18 were examined by ELISA on day 3 after I/R. (F) The expression of miR-21–5p and miR-331–5p was assessed by qRT-PCR on day 3 after I/R. N = 5 for the sham group, N = 8 for all other groups; *, $P < 0.05$; **, $P < 0.01$; ***, $P < 0.001$.

the culture medium was washed out, and 100 μl of DMSO (Sigma Aldrich) was added to each well. Ten minutes later, the absorbance at 490 nm was measured by a plate reader.

2.8. Quantitative real-time reverse transcription PCR (qRT-PCR)

Total RNA was extracted from BV2 cells and brain tissues with RNAiso Plus regent (Takara Bio, DaLian, China). A total of 1 g of total RNA was used to synthesize complementary DNA with Prime Script RT Master Mix (Takara Bio). Then, qRT-PCR was carried out using SYBR Green (Takara Bio) based on the manufacturer's protocol. U6 was used as an internal control. All primers used are listed as follows:

mouse miR-21–5p, forward, 5′- CGCGCTAGCTTATCAGACTGA -3′ and reverse, 5′- GTGCAGGGTCCGAGGT -3’;

mouse miR-331–5p, forward, 5′- GCGCTAGGTATGGTCCCAG -3′ and reverse, 5′- GTGCAGGGTCCGAGGT -3’;

mouse U6, forward, 5′- TCCGACGCCGCCATCTCTA -3′ and reverse, 5′- TATCGCACATTAAGCCTCTA -3’.

2.9. Western blot analysis

Cells and brain tissues were lysed in RIPA buffer containing 1% protease inhibitor and phosphatase inhibitor (Cwbio, Beijing, China). The lysates were centrifuged, and the supernatants were collected. Then, the protein concentrations of the samples were determined by a BCA kit (ThermoFisher Scientific). The protein samples were separated on 10% SDS-PAGE gels and then transferred to NC membranes (GE Healthcare, Madison, WI, USA). After blocking with 5% BSA for 2 h at room temperature, the membranes were then incubated with primary antibodies against TXNIP (14715, Cell Signaling Technology, Danvers, MA, USA), TRAF6 (ab227560, Abcam, Cambridge, MA, USA), p-p65 (ab53489, Abcam), p-65 (8242, Cell Signaling Technology), ASC (67824, Cell Signaling Technology), NLRP3 (15101, Cell Signaling Technology), cleaved caspase-1 (89332, Cell Signaling Technology) and GAPDH (5174, Cell Signaling Technology) at dilutions of 1:3000 at 4 °C overnight. Subsequently, the membranes were incubated with a secondary antibody (Cwbio, Beijing, China) at room temperature for 1 h. Finally, the signals were enhanced with an ECL detection kit (Pierce Biotechnology, Rockford, IL, USA).

2.10. Luciferase reporter assay

The 3’ UTR fragment of TXNIP, which contains putative miR-21–5p binding sites, and of TRAF6, which contains miR-331–5p binding sites, and respective mutant sites were synthesized by GenePharma (Shanghai, China). The mutagenesis of the binding sites in TXNIP and TRAF6 was achieved using the Site-Directed Mutagenesis Kit (Toyobo, Japan). These fragments were subcloned into the luciferase reporter gene vector. Different combinations of reporter plasmids with miR-21/miR-331 mimics and inhibitors and NC mimics and inhibitors were transfected into HEK-293T cells using Lipofectamine 3000 (Invitrogen, Carlsbad, CA, USA). Forty-eight hours later, luciferase activity was assessed with the Dual-Luciferase Reporter Assay System (Promega, Madison, WI, USA).

2.11. Measurement of IL-18 and IL-1β

IL-18 and IL-1β levels in the cerebrospinal fluid and the culture

medium of BV2 cells were assessed with an ELISA kit (ThermoFisher Scientific). The results were quantified by a microplate reader at an absorbance at 450 nm.

2.12. Statistical analyses

All data are expressed as the mean ± SD, and all analyses were performed with GraphPad Prism 7.0. A *t*-test was used for comparisons of two groups. One-way ANOVA followed by Tukey's post hoc test was used for multiple comparisons. $p < 0.05$ was considered statistically significant.

3. Results

3.1. MCAO inflammasome activation was induced, and miR-21–5p and miR-331–5p were downregulated in MCAO mice

First, MCAO was established to generate an *in vivo* model of ischaemia, and TTC staining was used to validate the stability and reproducibility of the model (Fig. 1A). The mNSS results demonstrated that the MCAO procedure induced neurological deficits in the mice (Fig. 1B). Moreover, H&E staining results further validated brain injury in the MCAO mice (Fig. 1C).

To explore whether ischaemia induces inflammasome activation, the levels of NLRP3 inflammasome-related proteins in brain tissues were detected by Western blot assay. Notably, compared with those in the sham mice, the levels of NLRP3 inflammasome components, including ASC, NLRP3 and cleaved caspase-1 (the active form of caspase-1), were significantly increased in MCAO mice (Fig. 1D). Since TXNIP and TRAF6 are well-established regulators of the NLRP3 inflammasome [1,16,26], we also examined their expression. We found that TXNIP and TRAF6 were both upregulated in MCAO mice (Fig. 1D). Inflammasome activation has been reported to cause membrane rupture, resulting in the release of pro-inflammatory cytokines, including IL-1β and IL-18. Hence, we also examined the levels of IL-1β and IL-18 in the cerebrospinal fluid. ELISA showed that the release of IL-1β and IL-18 was elevated in the cerebrospinal fluid of MCAO mice (Fig. 1E). In addition, PCR results demonstrated that miR-21–5p and miR-331–5p were downregulated in MCAO mice (Fig. 1F), implying their role in ischaemic injury.

Taken together, these results demonstrate that ischaemia induced inflammasome activation and downregulated miR-21–5p and miR-331–5p in MCAO mice.

3.2. Gastrodin combined with rhynchophylline alleviated ischaemia-induced inflammasome activation in vivo

Gastrodin and rhynchophylline both exert protective effects in ischaemia brain injury [13,18]. However, the effects of these two agents on ischaemia-induced inflammasome activation and the protective effects of the combination of these two agents in ischaemia-induced brain injury remain unclear. To investigate their effects, MCAO mice were administered gastrodin or rhynchophylline or both. Our TTC staining, mNSS and H&E staining results demonstrated that both gastrodin and rhynchophylline attenuated ischaemia-induced brain injury, while the combination of gastrodin and rhynchophylline further attenuated ischaemia-induced brain damage (Fig. 2A, B, C).

To investigate the effects of gastrodin and rhynchophylline on ischaemia-induced inflammasome activation, we examined the levels of ASC, NLRP3, cleaved caspase-1, TRAF6, and TXNIP, and the release of IL-1β and IL-18. We found that both gastrodin and rhynchophylline prevented ischaemia-induced increases in ASC, NLRP3, cleaved-caspase-1, IL-1β and IL-18, while their combination had stronger effects (Fig. 2D and E). Moreover, gastrodin alone and the combination attenuated ischaemia-induced elevation in TXNIP, while rhynchophylline alone had no effect (Fig. 2D). In contrast, rhynchophylline alone and the combination decreased the ischaemia-induced elevation in TRAF6, while gastrodin alone had no effect (Fig. 2D). Due to the regulatory effect of gastrodin on miR-21–5p and the regulatory effect of rhynchophylline on miR-331–5p [17,25], we investigated the expression of miR-21–5p and miR-331–5p. PCR results showed that only gastrodin and the combination of gastrodin and rhynchophylline restored the ischaemia-induced decreases in miR-21–5p, while only rhynchophylline alone and the combination restored the ischaemia-induced decreases in miR-331–5p (Fig. 2F).

Taken together, these results demonstrate that the combination of gastrodin and rhynchophylline alleviated ischaemia-induced brain injury and inflammasome activation in MCAO mice.

3.3. Gastrodin combined with rhynchophylline alleviated OGD-induced inflammasome activation in vitro

To further confirm the effects of gastrodin and rhynchophylline on ischaemia-induced inflammasome activation, we established an *in vitro* model of ischaemia in BV2 cells. As shown in Fig. 3A, OGD treatment time-dependently decreased the cell viability of BV2 cells. Consistent with the *in vivo* results, both gastrodin and rhynchophylline alleviated the OGD-induced decrease in cell viability, while their combination further restored cell viability (Fig. 3B). Additionally, both gastrodin and rhynchophylline prevented the OGD-induced increase in ASC, NLRP3, cleaved-caspase-1, and p-p65, and the release of IL-1β and IL-18, while their combination had stronger effects (Fig. 3C and D). Moreover, only gastrodin alone and the combination blocked the OGD-induced elevation in TXNIP, and only rhynchophylline alone and the combination blocked the OGD-induced elevation in TRAF6 (Fig. 3C). We also examined the expression of miR-21–5p and miR-331–5p by qRT-PCR. We found that only gastrodin alone and the combination blocked the OGD-induced decrease in miR-21–5p, and only rhynchophylline alone and the combination blocked the OGD-induced decrease in miR-331–5p (Fig. 3E).

Taken together, these results show that gastrodin combined with rhynchophylline alleviated OGD-induced inflammasome activation *in vitro*.

3.4. miR-21–5p directly binds to TXNIP, while miR-331–5p directly binds to TRAF6

The relationship between miR-21–5p and TXNIP and that between miR-331–5p and TRAF6 were investigated. According to Targetscan analysis, TXNIP was predicted to be a target of miR-21–5p, while TRAF6 was predicted to be a target of miR-331–5p (Fig. 4A and B). To validate whether TXNIP and TRAF6 are targets of miR-21–5p and miR-331–5p respectively, a luciferase assay was performed. As shown in Fig. 4C, a miR-21–5p inhibitor significantly increased luciferase activity in the WT-TXNIP group, while miR-21–5p mimics remarkably decreased luciferase activity in the WT-TXNIP group. In the MUT-TXNIP group, neither the miR-21–5p inhibitor nor miR-21–5p mimics affected luciferase activity. Meanwhile, a miR-331–5p inhibitor significantly increased luciferase activity in the WT-TRAF6 group, while miR-331–5p mimics remarkably decreased luciferase activity in the WT-TXNIP group (Fig. 4D). In the MUT-TRAF6 group, neither the miR-331–5p inhibitor nor miR-331–5p mimics affected luciferase activity (Fig. 4D).

Taken together, these results illustrate that TXNIP is a target gene of miR-21–5p and that TRAF6 is a target gene of miR-331–5p.

3.5. miR-21–5p overexpression combined with miR-331–5p overexpression suppressed OGD-induced inflammasome activation

To investigate the role of miR-21–5p and miR-331–5p in OGD-induced inflammasome activation, we transfected BV2 cells with miR-21–5p mimics, miR-331–5p mimics or both. As shown in Fig. 5A, miR-

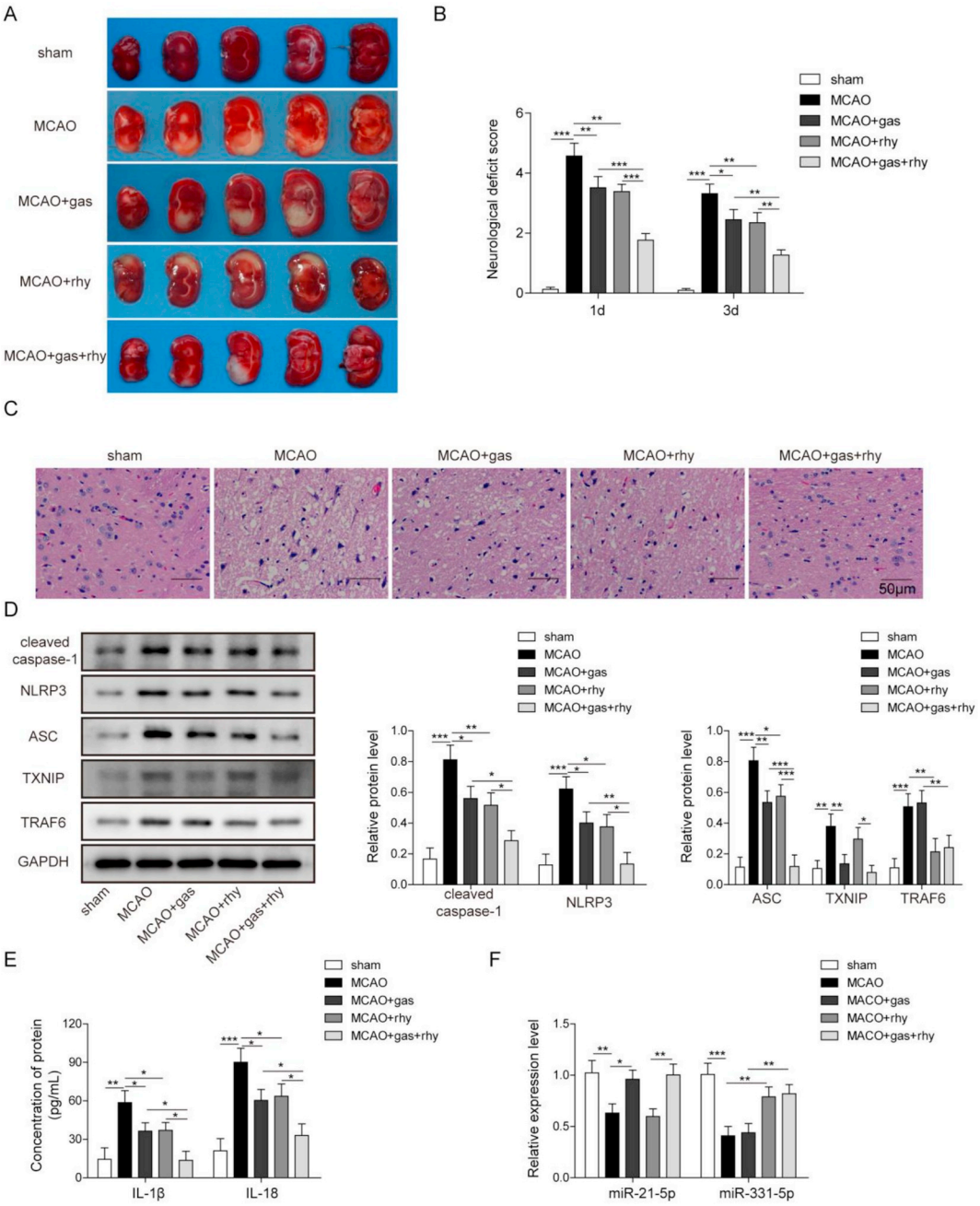

Fig. 2. The combination of gastrodin and rhynchophylline alleviated ischaemia-induced inflammasome activation. (A) Representative images of TTC staining of brain sections. Three days after I/R, brain sections were obtained for TTC staining. Gas, gastrodin; rhy, rhynchophylline. (B) The effect of gastrodin and/or rhynchophylline on neurological deficits were determined by the mNSS test. The mNSS test was carried out on days 1 and 3 after I/R. (C) Representative images of H &E staining of brain sections. Three days after I/R, brain sections were obtained for H&E staining. (D) The effect of gastrodin and/or rhynchophylline on the expression levels of TXNIP, TRAF6, caspase-1, NLRP3 and ASC was examined by Western blotting on day 3 after I/R. (E) The effect of gastrodin and/or rhynchophylline on the levels of IL-1β and IL-18 was examined by ELISA on day 3 after I/R. (F) The effect of gastrodin and/or rhynchophylline on the expression of miR-21–5p and miR-331–5p was assessed by qRT-PCR on day 3 after I/R. N = 5 for the sham group, N = 8 for all other groups; *, $P < 0.05$; **, $P < 0.01$; ***, $P < 0.001$.

21–5p mimics and the combination of miR-21–5p mimics and miR-331–5p mimics significantly increased the level of miR-21–5p, and miR-331–5p and the combination markedly increased the level of miR-331–5p. Similar to gastrodin and rhynchophylline, both miR-21–5p mimics and miR-331–5p mimics attenuated the OGD-induced decrease in cell viability and inflammasome activation, while their combination had more significant protective effects (Fig. 5B–D).

Taken together, these data suggest that miR-21–5p and miR-331–5p play a protective role in OGD-induced inflammasome activation in BV2 cells.

3.6. miR-21–5p and miR-331–5p mediated the protective effects of gastrodin and rhynchophylline in OGD-induced inflammasome activation

To determine whether gastrodin and rhynchophylline exert protective effects by modulating miR-21–5p and miR-331–5p, we transfected BV2 cells with a miR-21–5p inhibitor or a miR-331–5p inhibitor. q-PCR results validated that the miR-21 inhibitor suppressed the gastrodin-induced increase in miR-21 expression and that the miR-331 inhibitor suppressed the rhynchophylline-induced increase in miR-331 expression in OGD-treated BV2 cells (Fig. 6A). In OGD-treated BV2

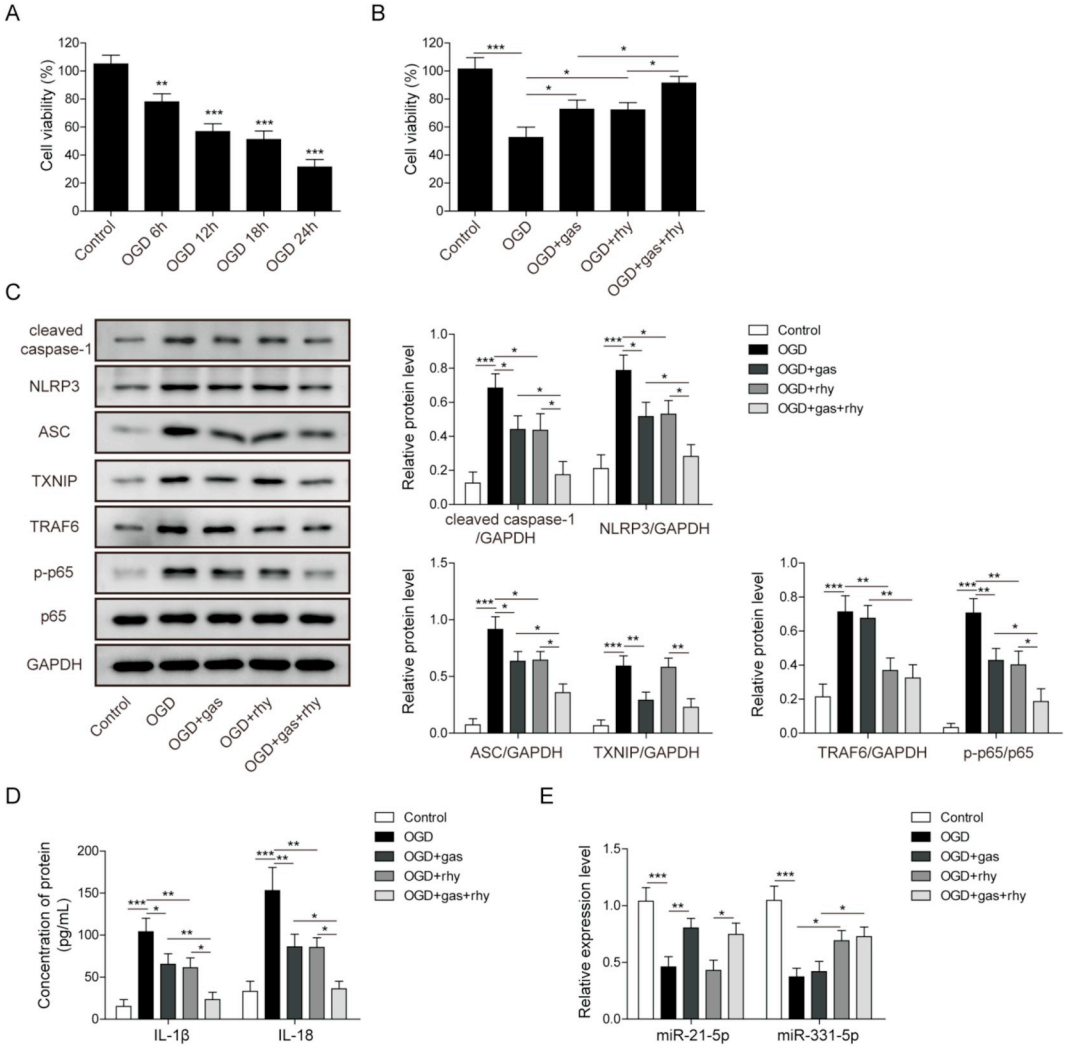

Fig. 3. The combination of gastrodin and rhynchophylline alleviated OGD-induced inflammasome activation in BV2 cells. (A) Cell viability was assessed by the MTT assay 6, 12, 18 and 24 h after OGD treatment. (B) The effect of gastrodin and/or rhynchophylline on cell viability was assessed by the MTT assay 12 h after OGD treatment. (C) The effect of gastrodin and/or rhynchophylline on the expression levels of TXNIP, TRAF6, cleaved caspase-1, NLRP3, p-p65 and ASC was examined by Western blotting 12 h after OGD treatment. (D) The effect of gastrodin and/or rhynchophylline and their combination on the levels of IL-1β and IL-18 in the culture medium was examined by ELISA 12 h after OGD treatment. (E) The effect of gastrodin and/or rhynchophylline and their combination on the expression of miR-21–5p and miR-331–5p was assessed by qRT-PCR 12 h after OGD treatment. In each experiment, the cells were treated with gastrodin and/or rhynchophylline after 1 h of OGD treatment. The data are shown as the mean ± SD based on at least three independent experiments. *, $P < 0.05$; **, $P < 0.01$; ***, $P < 0.001$.

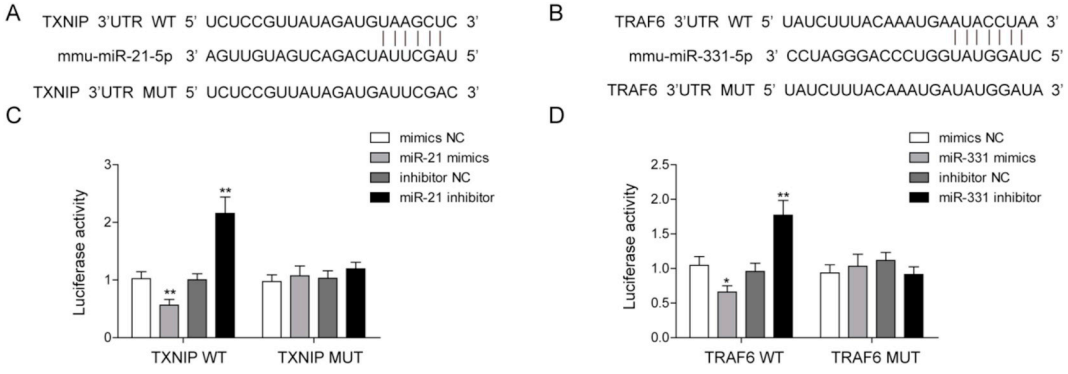

Fig. 4. miR-21–5p directly binds to TXNIP, while miR-331–5p directly binds to TRAF6. (A) The potential binding between miR-21–5p and TXNIP was predicted by Targetscan. (B) The potential binding between miR-331–5p and TRAF6 was predicted by Targetscan and validated by a luciferase reporter gene assay. (C) The binding between miR-21–5p and TXNIP was validated by a luciferase reporter gene assay. (D) The binding between miR-331–5p and TRAF6 was validated by a luciferase reporter gene assay. The data are shown as the mean ± SD based on at least three independent experiments. *, $P < 0.05$; **, $P < 0.01$.

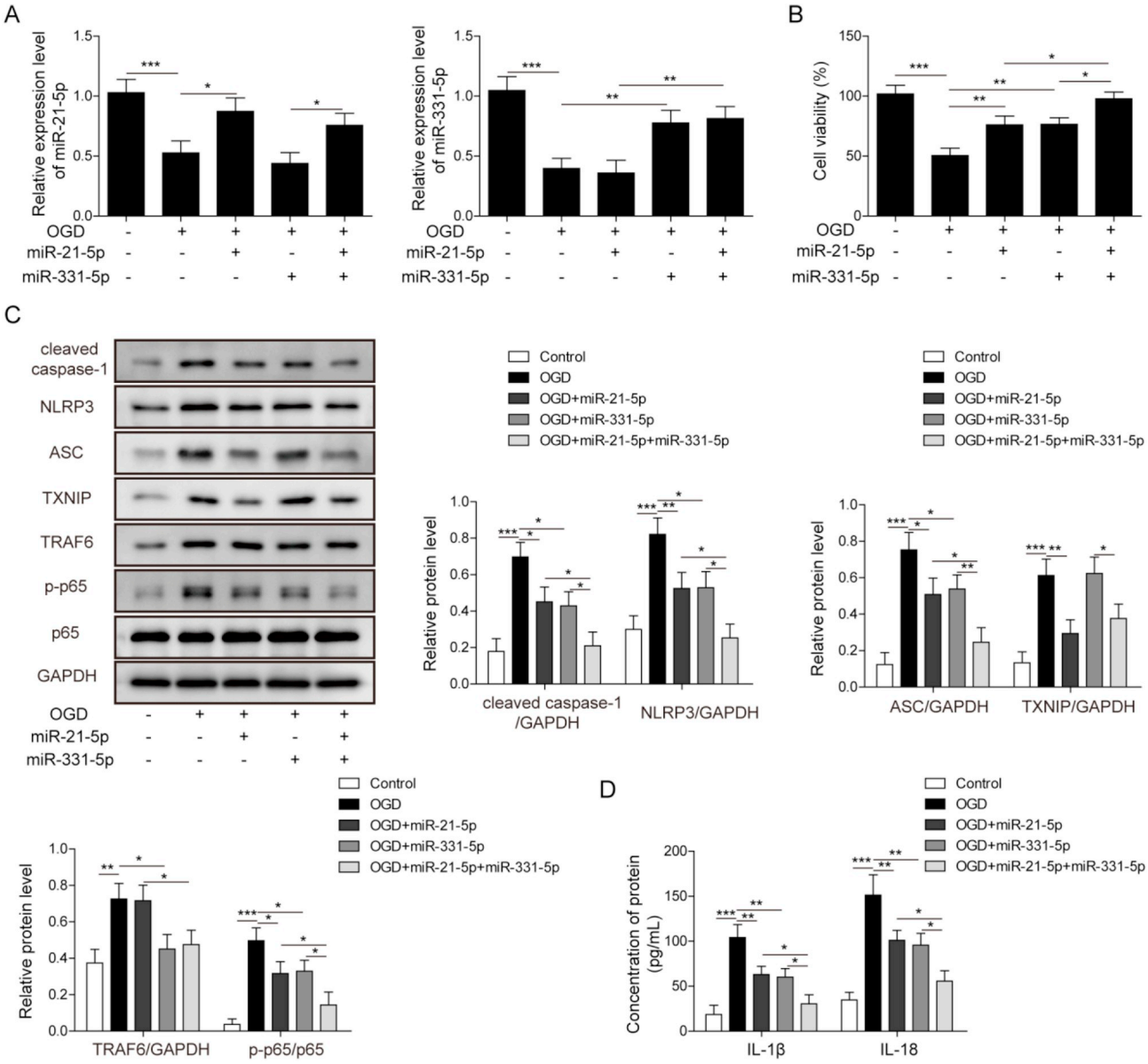

Fig. 5. Both miR-21–5p and miR-331–5p overexpression alleviated OGD-induced inflammasome activation in BV2 cells. (A) The expression of miR-21–5p and miR-331–5p after transfection with miR-21–5p mimics and/or miR-331–5p mimics was examined by qRT-PCR at 48 h after transfection. (B) The effect of miR-21–5p and miR-331–5p overexpression on cell viability was assessed by MTT assay at 12 h after OGD treatment. (C) The effect of miR-21–5p and miR-331–5p overexpression on the expression levels of TXNIP, TRAF6, caspase-1, NLRP3, p-p65 and ASC were examined by Western blot at 6 h after OGD treatment. (D) The effect of miR-21–5p and miR-331–5p overexpression on the levels of IL-1β and IL-18 in the culture medium was examined by ELISA at 6 h after OGD treatment. In each experiment, 48 h before OGD treatment, cells were transfected with miR-21–5p and/or miR-331–5p mimics. Data are shown as the mean ± SD based on at least three independent experiments. *, $P < 0.05$; **; $P < 0.01$; ***, $P < 0.001$.

cells, the miR-21–5p inhibitor completely reversed the protective effects of gastrodin on cell viability, and the miR-331–5p inhibitor completely blocked the protective effects of rhynchophylline on cell viability (Fig. 6B). Moreover, the miR-21–5p inhibitor abolished the alterations in ASC, NLRP3, cleaved caspase-1, TXNIP and p-p65 caused by gastrodin, and the miR-331–5p inhibitor abolished the decline in ASC, NLRP3, cleaved caspase-1, TRAF6 and p-p65 caused by rhynchophylline (Fig. 6C). In addition, the miR-21–5p inhibitor and miR-331–5p inhibitor reversed the decline in the release of IL-1β and IL-18 caused by gastrodin and rhynchophylline, respectively (Fig. 6D).

Taken together, these data suggest that miR-21–5p and miR-331–5p mediated the protective effects of gastrodin and rhynchophylline, respectively, in OGD-induced inflammasome activation.

3.7. The protective effect of the combination of gastrodin and rhynchophylline was comprised by the inhibition of miR-21–5p and miR-331–5p

To further verify whether miR-21–5p and miR-331–5p mediate the protective effects of the combination of gastrodin and rhynchophylline, a miR-21–5p inhibitor and miR-331–5p inhibitor were cotransfected into BV2 cells. As shown in Fig. 7A, the restoration of miR-21–5p levels caused by the combination of gastrodin and rhynchophylline in OGD-treated BV2 cells was reversed by the miR-21–5p inhibitor and the combination of the miR-21–5p inhibitor and the miR-331–5p inhibitor. Similarly, the restoration of miR-331–5p levels caused by the combination of gastrodin combined with rhynchophylline in OGD-treated BV2 cells was reversed by the miR-331–5p inhibitor and the

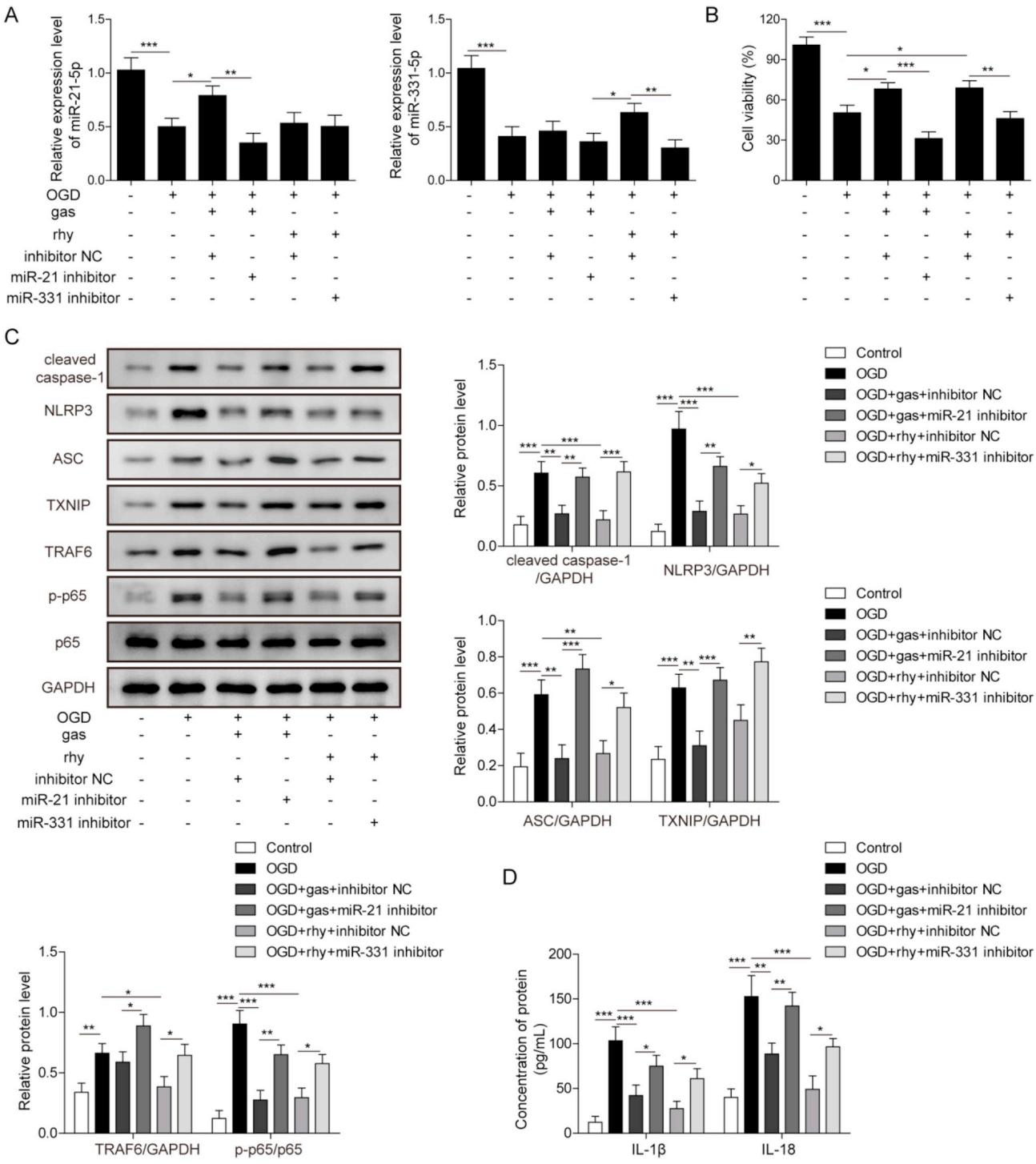

Fig. 6. A miR-21–5p and miR-331–5p inhibitor counteracted the protective effects of gastrodin and rhynchophylline in BV2 cells. (A) The expression of miR-21–5p and miR-331–5p was examined by qRT-PCR 12 h after OGD treatment. (B) Cell viability was assessed by the MTT assay 12 h after OGD. (C) The expression levels of TXNIP, TRAF6, caspase-1, NLRP3, p-p65 and ASC were examined by Western blotting 6 h after OGD. (D) The levels of IL-1β and IL-18 in the culture medium were examined by ELISA 12 h after OGD. Before OGD treatment, BV2 cells were transfected with inhibitors or NC for 48 h. In each experiment, the cells were treated with gastrodin and/or rhynchophylline after 1 h of OGD treatment. The data are shown as the mean ± SD based on at least three independent experiments. *, $P < 0.05$; **, $P < 0.01$; ***, $P < 0.001$.

combination of the miR-331-5 inhibitor and the miR-21–5p inhibitor (Fig. 7A). Our MTT results demonstrated that the increased cell viability caused by the combination of gastrodin and rhynchophylline was prevented by both the miR-21–5p and miR-331–5p inhibitor, while the combination of these two inhibitors further attenuated the survival-promoting effects of the combination of gastrodin and rhynchophylline in OGD-treated cells (Fig. 7B). Furthermore, the alterations in ASC, NLRP3, cleaved caspase-1, TXNIP and p-p65 caused by the combination of gastrodin and rhynchophylline were counteracted by both the miR-21–5p and miR-331–5p inhibitor in OGD-treated BV2 cells, while the combination of these two inhibitors completely blocked the alterations in the levels of these proteins (Fig. 7C). In addition, the release of IL-1β

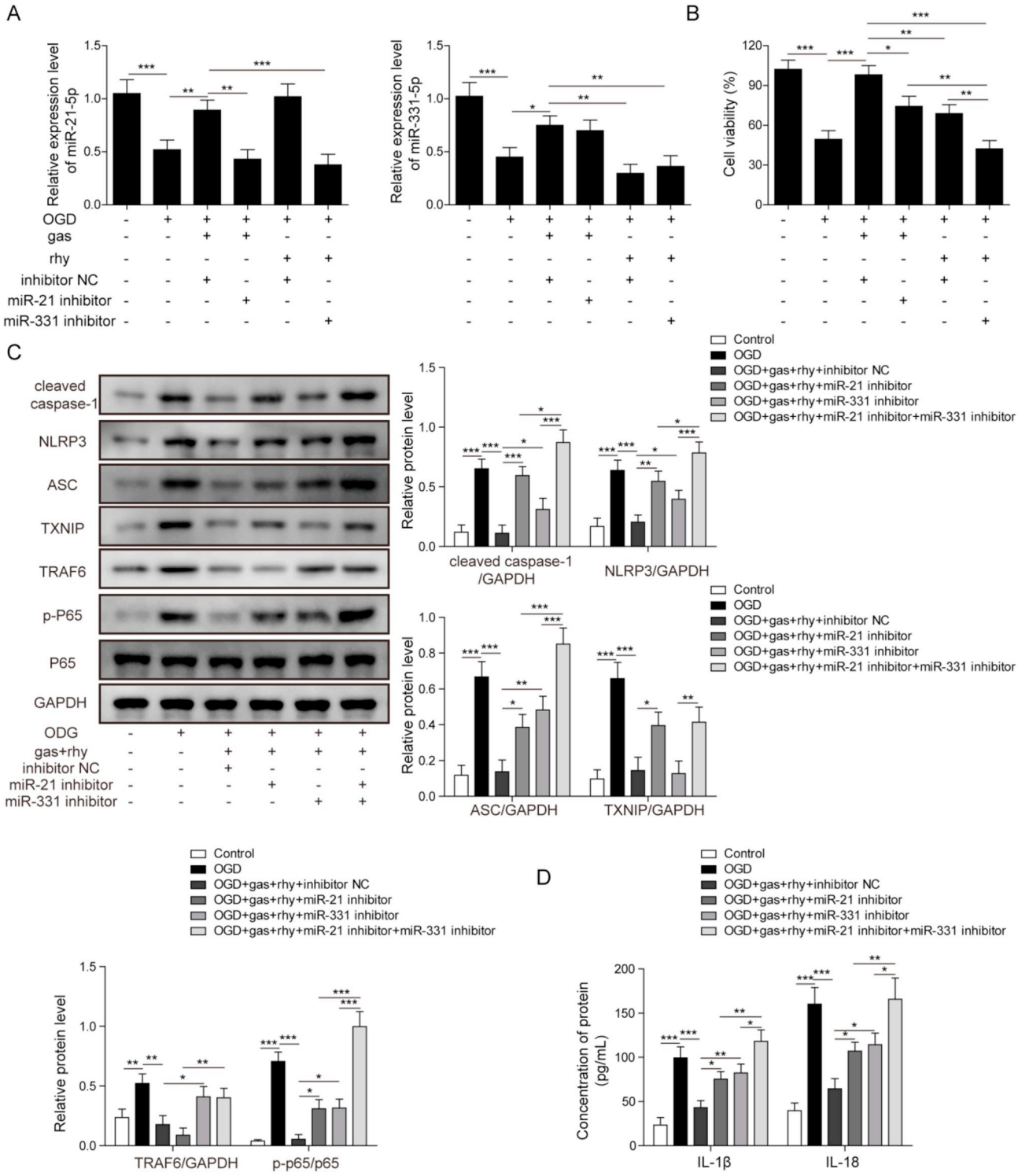

Fig. 7. The combination of the miR-21–5p and miR-331–5p inhibitors blocked the synergistic protective effects of gastrodin and rhynchophylline in OGD-treated BV2 cells. (A) The expression of miR-21–5p and miR-331–5p was examined by qRT-PCR 12 h after OGD treatment. (B) Cell viability was assessed by the MTT assay 12 h after OGD. (C) The expression levels of TXNIP, TRAF6, caspase-1, NLRP3, p-p65 and ASC were examined by Western blotting 6 h after OGD. (D) The levels of IL-1β and IL-18 in the culture medium were examined by ELISA 12 h after OGD. Before OGD treatment, BV2 cells were cotransfected with inhibitors or NC for 48 h. In each experiment, the cells were treated with gastrodin and rhynchophylline after 1 h of OGD treatment. The data are shown as the mean ± SD based on at least three independent experiments. *, $P < 0.05$; **, $P < 0.01$; ***, $P < 0.001$.

and IL-18 was also examined in cells co-transfected with the miR-21–5p and miR-331–5p inhibitors. As shown in Fig. 7D, both the miR-21–5p inhibitor and miR-331–5p inhibitor attenuated the decreased release of IL-1β and IL-18 caused by the combination of gastrodin and rhynchophylline, while the combination of these two inhibitors completely restored the release of IL-1β and IL-18 in OGD-treated cells.

Taken together, these data suggest that the protective effect of the combination of gastrodin and rhynchophylline was mediated by miR-21–5p and miR-331–5p.

4. Discussion

NLRP3 inflammasome-induced inflammatory responses play a vital role in ischaemia-induced brain damage [10,22]. Therefore, inhibiting the NLRP3 inflammasome could be a promising strategy for ischaemic stroke. In the present study, we investigated whether the combination of gastrodin and rhynchophylline is effective in inhibiting the NLRP3 inflammasome in ischaemia. Our data demonstrated that gastrodin combined with rhynchophylline exerts protective effects in ischaemic stroke by suppressing NLRP3 inflammasome activation through a two-pronged mechanism: 1) gastrodin upregulates miR-21–5p, which downregulates TXNIP, a positive regulator of the NLRP3 inflammasome, and 2) rhynchophylline upregulates miR-331–5p, which suppresses the NLRP3 inflammasome by targeting the TRAF6/NF-κB pathway. To our knowledge, this is the first report regarding the synergistic protective effect of gastrodin and rhynchophylline in ischaemia-induced pyroptosis, and it thus suggests a novel method for ameliorating ischaemia-induced cerebral injury.

Several studies have highlighted the protective effects of gastrodin and rhynchophylline in ischaemia-induced injury. Gastrodin mitigates ischaemia brain damage by decreasing reactive oxidative stress and suppressing inflammation [23]. Rhynchophylline has been reported to mitigate ischaemia injury by acting on neurotransmitter receptors [15]. However, these reports do not address the question of whether gastrodin and rhynchophylline regulate ischaemia-induced inflammasome activation. Our study is the first to report the synergistic protective effects of gastrodin and rhynchophylline and their suppressive effects on NLRP3 inflammasome activation. The synergistic effect of gastrodin and rhynchophylline on inflammasome activation is not surprising because gastrodin and rhynchophylline function through the miR-21–5p/TXNIP and miR-331–5p/TRAF6/NF-κB pathways, respectively. Interestingly, although gastrodin does not regulate the expression of TRAF6, it does block NF-κB subunit p65 phosphorylation. This result is consistent with a previous study reporting the ability of gastrodin to suppress the inflammatory response by inactivating NF-κB [28].

miR-21–5p, one of the most intensively studied microRNAs, has long been recognized as a positive regulator in ischaemic injury. miR-21–5p suppresses microglia-induced neurotoxicity by inhibiting Fasl in ischaemia [30]. The forced expression of miR-21–5p reduces neuronal apoptosis by downregulating FASLG [6]. Moreover, miR-21–5p has been identified as a regulator of the immune response due to its interaction with TLR4 [4]. Thus, it is not surprising that miR-21–5p regulates NF-κB independently of TRAF6. Compared with that of miR-21–5p, little is known about the role of miR-331–5p in ischaemia. The only report regarding miR-331–5p in ischaemia suggests that miR-331–5p might mediate its neuroprotective effect after valproic acid-induced insult in MCAO rats [14]. Our study indicates that miR-331–5p might be a new target for ischaemic stroke due to its regulatory role on the NLRP3 inflammasome via targeting TRAF6.

5. Conclusion

In summary, our study confirms the synergistic protective effects of gastrodin and rhynchophylline in ischaemia-induced brain damage. Our study also identifies the underlying mechanism: gastrodin suppresses inflammasome activation and exerts a protective effect by regulating the miR-21–5p target TXNIP, while rhynchophylline suppresses inflammasome activation and exerts a protective effect by regulating the miR-331–5p target TRAF6. The protective effect of the combination of gastrodin and rhynchophylline in ischaemia-induced brain damage makes the combination an attractive candidate for ischaemic stroke treatment. However, more clinical experiments are warranted to support our results.

Declaration of competing interest

We declare that we have no conflicts of interest.

Acknowledgements

Not applicable.

References

[1] J.M. Abais, M. Xia, G. Li, Y. Chen, S.M. Conley, T.W. Gehr, P.-L. Li, Nod-like receptor protein 3 (NLRP3) inflammasome activation and podocyte injury via thioredoxin-interacting protein (TXNIP) during hyperhomocysteinemia, J. Biol. Chem. 289 (39) (2014) 27159–27168.
[2] V. Ambros, The functions of animal microRNAs, Nature 431 (7006) (2004) 350.
[3] J. Anrather, C. Iadecola, Inflammation and stroke: an overview, Neurotherapeutics 13 (4) (2016) 661–670.
[4] R.E. Barnett, D.J. Conklin, L. Ryan, R.C. Keskey, V. Ramjee, E.A. Sepulveda, W.G. Cheadle, Anti-inflammatory effects of miR-21 in the macrophage response to peritonitis, J. Leukoc. Biol. 99 (2) (2016) 361–371.
[5] T. Bergsbaken, S.L. Fink, A.B. den Hartigh, W.P. Loomis, B.T. Cookson, Coordinated host responses during pyroptosis: caspase-1–dependent lysosome exocytosis and inflammatory cytokine maturation, J. Immunol. 187 (5) (2011) 2748–2754.
[6] B. Buller, X. Liu, X. Wang, R.L. Zhang, L. Zhang, A. Hozeska-Solgot, Z.G. Zhang, MicroRNA-21 protects neurons from ischemic death, FEBS J. 277 (20) (2010) 4299–4307.
[7] Á. Chamorro, U. Dirnagl, X. Urra, A.M. Planas, Neuroprotection in acute stroke: targeting excitotoxicity, oxidative and nitrosative stress, and inflammation, Lancet Neurol. 15 (8) (2016) 869–881.
[8] N. Chen, S. Chu, X. Zhou, C. Chen, Z. Zhang, Ginsenoside Rg1 protects against ischemic/reperfusion-induced neurotoxicity through miR-144/Nrf2/ARE pathway, FASEB J. 33 (1_supplement) (2019) 500.514-500.514.
[9] A. Denes, E. Pinteaux, N.J. Rothwell, S.M. Allan, Interleukin-1 and stroke: biomarker, harbinger of damage, and therapeutic target, Cerebrovasc. Dis. 32 (6) (2011) 517–527.
[10] D.Y.-W. Fann, S. Lee, S. Manzanero, S.-C. Tang, M. Gelderblom, P. Chunduri, J. Thundyil, Intravenous immunoglobulin suppresses NLRP1 and NLRP3 inflammasome-mediated neuronal death in ischemic stroke, Cell Death Dis. 4 (9) (2013) e790.
[11] V.L. Feigin, B. Norrving, G.A. Mensah, Global burden of stroke, Circ. Res. 120 (3) (2017) 439–448.
[12] S.M. Hammond, An overview of microRNAs, Adv. Drug Deliv. Rev. 87 (2015) 3–14.
[13] H. Huang, R. Zhong, Z. Xia, J. Song, L. Feng, Neuroprotective effects of rhynchophylline against ischemic brain injury via regulation of the Akt/mTOR and TLRs signaling pathways, Molecules 19 (8) (2014) 11196–11210.
[14] J.G. Hunsberger, E.B. Fessler, Z. Wang, A.G. Elkahloun, D.-M. Chuang, Post-insult valproic acid-regulated microRNAs: potential targets for cerebral ischemia, Am. J. Tourism Res. 4 (3) (2012) 316.
[15] T.-H. Kang, Y. Murakami, H. Takayama, M. Kitajima, N. Aimi, H. Watanabe, K. Matsumoto, Protective effect of rhynchophylline and isorhynchophylline on in vitro ischemia-induced neuronal damage in the hippocampus: putative neurotransmitter receptors involved in their action, Life Sci. 76 (3) (2004) 331–343.
[16] T. Lane, B. Flam, R. Lockey, N. Kolliputi, TXNIP shuttling: missing link between oxidative stress and inflammasome activation, Front. Physiol. 4 (2013) 50.
[17] C. Li, G. Tu, C. Luo, Y. Guo, M. Fang, C. Zhu, W. Liu, Effects of rhynchophylline on the hippocampal miRNA expression profile in ketamine-addicted rats, Prog. Neuro Psychopharmacol. Biol. Psychiatry 86 (2018) 379–389.
[18] B. Liu, F. Li, J. Shi, D. Yang, Y. Deng, Q. Gong, Gastrodin ameliorates subacute phase cerebral ischemia-reperfusion injury by inhibiting inflammation and apoptosis in rats, Mol. Med. Rep. 14 (5) (2016) 4144–4152.
[19] Y. Liu, J. Gao, M. Peng, H. Meng, H. Ma, P. Cai, G. Si, A review on central nervous system effects of gastrodin, Front. Pharmacol. 9 (2018) 24.
[20] E.Z. Longa, P.R. Weinstein, S. Carlson, R. Cummins, Reversible middle cerebral artery occlusion without craniectomy in rats, Stroke 20 (1) (1989) 84–91.
[21] R. Mao, Y. Fan, Y. Mou, H. Zhang, S. Fu, J. Yang, TAK1 lysine 158 is required for TGF-β-induced TRAF6-mediated Smad-independent IKK/NF-κB and JNK/AP-1 activation, Cell. Signal. 23 (1) (2011) 222–227.
[22] L. Minutoli, D. Puzzolo, M. Rinaldi, N. Irrera, H. Marini, V. Arcoraci, F. Squadrito, ROS-mediated NLRP3 Inflammasome Activation in Brain, Heart, Kidney, and Testis Ischemia/reperfusion Injury. Oxidative Medicine and Cellular Longevity, 2016, (2016).
[23] Z. Peng, S. Wang, G. Chen, R. Liu, J. Deng, J. Liu, C. Hai, Gastrodin alleviates cerebral ischemic damage in mice by improving anti-oxidant and anti-inflammation activities and inhibiting apoptosis pathway, Neurochem. Res. 40 (4) (2015) 661–673.
[24] Ø. Sandanger, T. Ranheim, L.E. Vinge, M. Bliksøen, K. Alfsnes, A.V. Finsen, G. Christensen, The NLRP3 inflammasome is up-regulated in cardiac fibroblasts and mediates myocardial ischaemia–reperfusion injury, Cardiovasc. Res. 99 (1) (2013) 164–174.
[25] Y. Xing, L. Li, Gastrodin protects rat cardiomyocytes H9c2 from hypoxia-induced injury by up-regulation of microRNA-21, Int. J. Biochem. Cell Biol. 109 (2019) 8–16.
[26] Y. Xing, X. Yao, H. Li, G. Xue, Q. Guo, G. Yang, G. Meng, Cutting edge: TRAF6

mediates TLR/IL-1R signaling–induced nontranscriptional priming of the NLRP3 inflammasome, J. Immunol. 199 (5) (2017) 1561–1566.
[27] F. Yang, Z. Wang, X. Wei, H. Han, X. Meng, Y. Zhang, Q. Pang, NLRP3 deficiency ameliorates neurovascular damage in experimental ischemic stroke, J. Cereb. Blood Flow Metab. 34 (4) (2014) 660–667.
[28] P. Yang, Y. Han, L. Gui, J. Sun, Y.-l. Chen, R. Song, L. Sun, Gastrodin attenuation of the inflammatory response in H9c2 cardiomyocytes involves inhibition of NF-κB and MAPKs activation via the phosphatidylinositol 3-kinase signaling, Biochem. Pharmacol. 85 (8) (2013) 1124–1133.
[29] Z.-B. Yang, X.-J. Luo, K.-D. Ren, J.-J. Peng, B. Tan, B. Liu, X. Ren, Beneficial effect of magnesium lithospermate B on cerebral ischemia–reperfusion injury in rats involves the regulation of miR-107/glutamate transporter 1 pathway, Eur. J. Pharmacol. 766 (2015) 91–98.
[30] L. Zhang, L.Y. Dong, Y.J. Li, Z. Hong, W.S. Wei, miR-21 represses FasL in microglia and protects against microglia-mediated neuronal cell death following hypoxia/ischemia, Glia 60 (12) (2012) 1888–1895.
[31] J. Zhou, S. Zhou, Antihypertensive and neuroprotective activities of rhynchophylline: the role of rhynchophylline in neurotransmission and ion channel activity, J. Ethnopharmacol. 132 (1) (2010) 15–27.
[32] R. Zhou, A. Tardivel, B. Thorens, I. Choi, J. Tschopp, Thioredoxin-interacting protein links oxidative stress to inflammasome activation, Nat. Immunol. 11 (2) (2010) 136.